Effects of Oxide Promoters on Metal Dispersion and Metal−Support Interactions in Ni Catalysts Supported on Activated Carbon

ARTICLE *in* INDUSTRIAL & ENGINEERING CHEMISTRY RESEARCH · DECEMBER 1997

Impact Factor: 2.59 · DOI: 10.1021/ie9703604 · Source: OAI

2 AUTHORS:

Shaobin Wang
Curtin University
269 PUBLICATIONS **9,268** CITATIONS

SEE PROFILE

Max Lu
University of Queensland
580 PUBLICATIONS **30,228** CITATIONS

SEE PROFILE

Effects of Oxide Promoters on Metal Dispersion and Metal−Support Interactions in Ni Catalysts Supported on Activated Carbon

Shaobin Wang and G. Q. (Max) Lu*

Department of Chemical Engineering, The University of Queensland, St. Lucia, Queensland 4072, Australia

Various oxide-promoted Ni catalysts supported on activated carbon were prepared, and the effect of promoters on the surface structure and properties of Ni catalysts was studied. Physical adsorption (N_2 adsorption), thermogravimetric analysis (TGA), temperature-programmed desorption (TPD), X-ray diffraction (XRD), and X-ray photoelectron spectroscopy (XPS) were used to characterize the catalysts. It is found that nickel is fairly uniformly distributed in the pores of the carbon support. Addition of promoters produces a more homogeneous distribution of nickel ion in carbon. However, distributions of promoters in the pores are varying. Addition of promoters increases the dispersion of nickel in carbon. Promoters also change the interaction between the carbon and Ni, resulting in significantly different behaviors of catalysts under various environments. CaO and MgO promoters improve the reactivity of nickel catalysts with O_2 but retard the interaction between nickel oxide and carbon. La_2O_3 shows some inhibiting effect on the interactions between nickel oxide and oxygen as well as carbon.

1. Introduction

Activated carbon is widely used as a catalyst support in recent years. In contrast to inorganic carriers, it has a number of advantages. One is the relatively facile recovery of the active phases, which is important for precious metals. The second is the modified surface characteristics, which can affect the catalyst activity. The third is its porous structure, which enables the formation of a highly dispersed metal phase.

Nickel catalysts are commonly used in many industry processes such as hydrogenation, hydrogenolysis of hydrocarbons, and steam reforming. A lot of researches have been reported on the characteristics and behavior of Ni catalysts, which are frequently supported on different metal oxides. There are a few papers on the study of Ni catalysts supported on activated carbon (Domingo-Garcia et al., 1994; Gandia and Montes, 1994; Haga et al., 1992; Wang and Lu, 1997).

One of the most interesting aspects in the field of heterogeneous catalysis is the study of promoters on catalytic activity and selectivity. The use of high surface area active carbon as a catalyst support seems attractive for studying the effects of metal oxide promoters on highly dispersed metal phases, since the metal−carbon interaction is very weak, thus favoring the metal−promoter interaction (Rodriguez-Ramos et al., 1989).

The present work aims to study the effect of MgO, CaO, and La_2O_3 promoters on the properties of nickel catalysts supported on activated carbon using various techniques, such as N_2 adsorption, X-ray photoelectron spectroscopy (XPS), X-ray diffraction (XRD), thermogravimetric analysis (TGA), and temperature-programmed desorption (TPD).

2. Experimental Section

2.1. Catalyst Preparation. A commercial activated carbon obtained from the Calgon Carbon Corp. (4 × 6 mm pellet) was used in this study. It was first treated with HCl and HF solution in order to remove inorganic impurities in it. After washing and drying in 103−105 °C overnight, it was ready for catalyst preparation. Nickel nitrate ($Ni(NO_3)_2 \cdot 6H_2O$) supplied by BDH Chemicals was loaded on the activated carbon sample by impregnation from an aqueous solution. In preparation of the promoted catalysts, magnesium nitrate (AJAX Chemicals), calcium nitrate (AJAX Chemicals), or lanthanum nitrate (BDH Chemicals) was added with nickel nitrate to the carbon supports by a simultaneous impregnation method. The nickel loading was set at 5%, while the promoter content was kept at 2%.

2.2. Characterization of Catalysts. The surface properties such as surface area, average pore radius, and pore volume were determined using a gas sorption analyzer (Quantachrome, NOVA 1200) using N_2 absorption at −196 °C. Before analysis, samples were degassed under vacuum for 3 h at 300 °C.

From the adsorption isotherm, surface area was determined using the BET equation. The total pore volume was derived from the amount of adsorption at a relative pressure close to unity, assuming that the pores were totally filled with the liquid adsorbate. The micropore volume was calculated from the adsorption isotherm using the Dubinin−Radushkevich equation, and the mesopore volume was determined by subtracting the micropore volume from the total pore volume. The average pore size was estimated from the pore volume, assuming a cylindrical pore geometry using the equation $R_p = 2V_{liq}/S$, where V_{liq} is the volume of liquid adsorbate contained in the pores and S is the BET surface area.

The micropore size distribution was obtained as follows. N_2 adsorption data on a nonporous carbon were used to evaluate t values at various relative pressures, P/P_0 (Kaneko et al., 1992). The comparison plots, t plots, were constructed by plotting the adsorbed amount V_a versus t at various relative pressures. The modified micropore method (MP) was then used to calculate the pore size distribution. More details can be found elsewhere (Zhu et al., 1997).

Thermogravimetric analysis (TGA) experiments were carried out in a thermobalance (Shimadzu TGA-50). Two series of experiments were made with either dry air or nitrogen. Samples were loaded into a platinum pan, heated in an air or N_2 atmosphere from ambient

* Author to whom correspondence is addressed. E-mail: maxlu@cheque.uq.edu.au. Phone: 61 7 33653735. Fax: 61 7 33654199.

S0888-5885(97)00360-6 CCC: $14.00

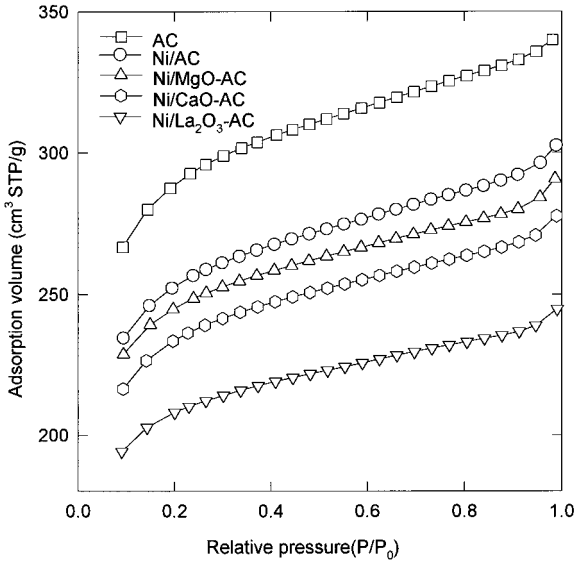

Figure 1. N_2 adsorption isotherms of the support and Ni catalysts at −196 °C.

temperature to 110 °C, held at this temperature for 30 min, and then heated to 750 °C at a heating rate of 10 °C/min.

Temperature-programmed desorption (TPD) experiments were carried out in a vertical tube furnace. A 0.5 g sample was placed in a quartz tube with He as the carrier gas at a flow rate of 30 mL/min. After heating to 110 °C and keeping this temperature for 60 min, the temperature was raised at 5 °C/min to 800 °C. The gases evolved during the TPD runs were continuously analyzed using a gas chromatograph (Shimaduz GC-17A) equipped with a thermal conductivity detector and a Carbosphere column.

XPS measurements were performed on a PHI-560 ESCA surface analysis system (Perkin-Elmer). The excitation source was the Mg Kα line ($h\gamma = 1253.6$ eV). The analysis chamber was maintained below 5×10^{-7} Torr during data acquisition. Either 50 or 100 eV regions of the photoelectrons of interest were scanned in ΔE = constant mode.

XRD patterns were obtained with a Philips PW 1840 powder diffractometer. Co Kα radiation was employed, covering 2θ between 2° and 90°. The mean crystallite diameters were estimated from application of the Scherrer equation (Lemaitre et al., 1985).

3. Results and Discussion

3.1. Structure Variation of Catalysts. Figure 1 shows the adsorption isotherms of the carbon support, unpromoted and promoted Ni catalysts. All adsorption isotherms are similar to a type I isotherm. Impregnation resulted in a decrease in the amount adsorbed, with only slight modification of the knee corresponding to microporosity.

A more quantitative comparison of the variation of the textural structure of the carbon support and nickel catalysts is given in Table 1. Impregnation of nickel nitrate on the support decreased its surface area and total pore volume. Addition of promoted oxides led to much lower S_{BET} and V_{total} in promoted nickel catalysts. However, the pore radii of the catalysts were slightly increased by impregnation, but the variations were negligible and well within experimental errors. This result is different from that reported by Molina-Sabio et al. (1994). They found that impregnation of activated carbon produced decreases in micropore and mesopore volumes as well as its mean pore size.

Table 1. Characterization of Catalyst Pore Structure[a]

catalyst	S_{BET} (m^2/g)	R (Å)	V_{total} (mL/g)	V_{micro} (mL/g)	V_{meso} (mL/g)
AC	984	11.30	0.556	0.435	0.121
Ni/AC	857	11.53	0.494	0.387	0.107
Ni/MgO−AC	826	11.38	0.470	0.373	0.097
Ni/CaO−AC	790	11.54	0.456	0.359	0.097
Ni/La_2O_3−AC	668	11.32	0.378	0.294	0.084

[a] R: average pore radius.

Table 2. Effect of Impregnation on the Decrease in Pore Volume

catalyst	V_{micro} (%)	V_{meso} (%)
Ni/AC	11.0	11.6
Ni/MgO−AC	14.2	20.0
Ni/CaO−AC	17.5	20.0
Ni/La_2O_3−AC	32.4	32.2

To evaluate the loss of pore volume by impregnation, the volume reductions in micropores and mesopores were calculated (Table 2). Pore volume decreased consistently in the micropores and mesopores for Ni/AC and Ni/La_2O_3−AC (activated carbon) catalysts. However, for samples Ni/MgO−AC and Ni/CaO−AC, impregnation resulted in more blocking of the mesopores. Tripathi and Ramachandran (1982) studied the pore structure of impregnated activated carbon and found that impregnates affected micro- and mesopores, reducing the total pore volume. Other researchers showed that impregnation produced a partial blocking of the porosity of the carbon, which was dependent on the original pore size distribution. If the carbon had a relatively significant mesoporosity, the loss of microporosity was more pronounced than that in essentially microporous carbons (Molina-Sabio et al., 1994).

In Figure 2 is shown the pore size distributions of the carbon support and various catalysts. It is seen that the support and catalysts show less difference in the range of micropore size distribution (before 10 Å). However, the pore size distributions in the range of 10−20 Å are quite different. In the range of supermicropore (>8 Å), there is a peak shift for the catalysts toward smaller pore sizes. The pore size is centered at 12.8 and 17 Å for the support, but they are centered at 11.8 and 16.5 Å, respectively, for the catalysts. These variations indicate that more pores are blocked in supermicropores for catalysts, especially for the promoted catalysts.

From the above results, it is deduced that nickel nitrate impregnate is possibly distributed uniformly in the pore or on the surface of the carbon support when impregnated, which shows about the same decreases in micropore and mesopore volume for the Ni/AC catalyst. Addition of promoters of $Mg(NO_3)_2$, $Ca(NO_3)_2$, and $La(NO_3)_3$ during the coimpregnation process altered the deposition behavior of $Ni(NO_3)_2$. It increased the amount of nickel nitrate deposition in the micropores. However, these promoters also showed a different distribution in carbon pores. Most of them deposited on the surface, resulting in more reduction in mesopore volume for Ni/MgO−AC and Ni/CaO−AC catalysts. For Ni/La_2O_3−AC catalyst, on the one hand, due to the synergistic effect of two impregnates more nickel salt was deposited in micropores of carbon; on the other hand, larger lanthanum ions were easily impregnated on the outer surface of carbon. In this way, the same levels of reduction in micropore and mesopore volumes resulted.

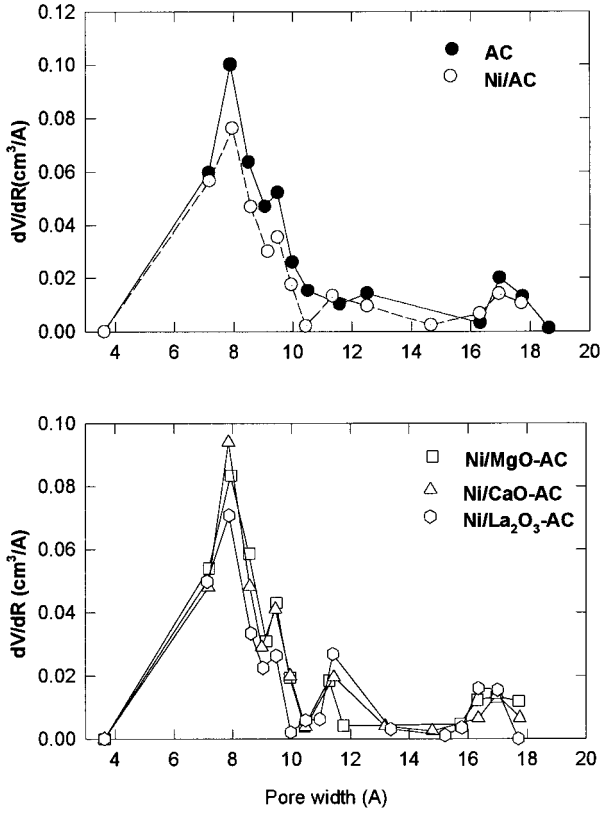

Figure 2. Micropore size distributions of carbon support and catalysts.

All these conclusions can be further substantiated by XPS results (discussed later).

3.2. Distribution and Dispersion of the Active Phase in Catalysts. The XPS technique provides valuable information on the location and distribution of the metal and promoter oxides in the pore structure of carbon. It has been found that Ni distribution may differ among various carbons depending on the structure and properties. Acidic treatment resulted in a more homogeneous distribution of Ni in carbon pores (Wang and Lu, 1997). Bekyarova and Mehandjiev (1996) also reported that most of the active phase (Ni) was in the pores of the Ni/AC catalysts and a small amount was on the surface. Figure 3 shows the Ni/C molar ratio correlation between the surface and bulk concentration. It is seen that the XPS Ni/C ratio increases with increasing Ni content of the catalysts. This is indicative of uniform dispersion of Ni throughout the carbon support.

In Table 3, the XPS metal/C and promoter/C ratios of various Ni catalysts are presented. It is shown that the surface nickel loadings are generally lower than their bulk content, especially for the Ni/La_2O_3−AC catalyst, in which the surface nickel is only one-third of its bulk content. This indicates that in all catalysts nickel is much more uniformly distributed within the carbon pores and is difficult to detect. The effect of promoter seems to increase the metal distribution in the carbon supports. The order of such a promotion is La_2O_3 > MgO > CaO.

For different promoters, the ratios of the surface MO/C to the bulk MO/C are varying. The MgO-promoted catalyst displays a much lower $(MO/C)_{xps}/(MO/C)_b$ ratio (<<1), whereas the ratios for Ni/CaO−AC and Ni/La_2O_3−AC catalysts are greater than 1. These data indicate that MgO is dispersed in the inner pores while

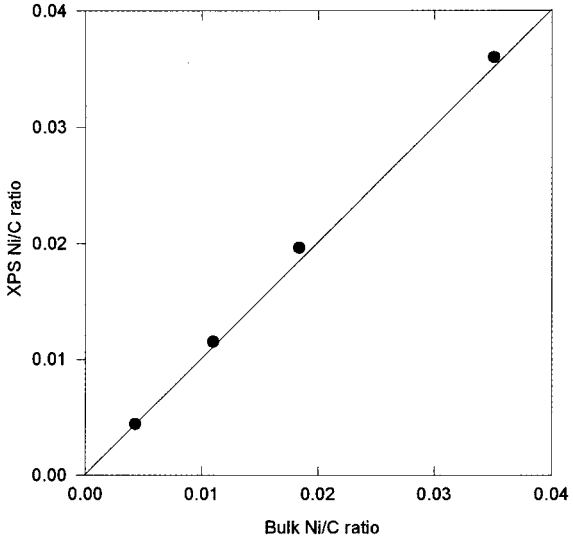

Figure 3. Comparison between Ni/C ratios on the surface and in the bulk.

CaO and La_2O_3 are concentrated on the outer surface. Rodriguez-Ramos et al. (1989) studied the effect of promoters on the surface characteristics of carbon-supported Co and Ru catalysts and found that oxide promoters (MgO, CeO_x, and V_2O_x) were mostly deposited on the surface of carbon.

From the above results it can be concluded that the locations of the metal and oxide promoters are altered during the impregnation process and the oxide promoters are mostly concentrated on the outer layer of the carbon supports while the metal is generally dispersed in the carbon pores. Addition of promoters results in a more uniform distribution of Ni in carbons because they quickly deposited in the pore mouth region when impregnated, possibly forcing nickel ions to move into the inner pores.

From the analysis of binding energy (BE) values of carbon and oxygen, we found that there exist BE peak shifts on C 1s and O 1s among the unpromoted and promoted nickel catalysts (Figure 4). In the case of C 1s, the peaks of Ni/AC and AC are at the same position and the peak shows a shift toward lower BE for promoted catalysts. This means that impregnation of nickel nitrate does not influence the surface complex properties of the carbon support and that promoters, however, have an effect on carbon properties, leading to higher graphitic and aromatic carbon complexes on carbon supports. Comparing the O 1s maximum shifts, we can infer the acid−base property of the carbon surface. It can be seen from Figure 4 that MgO and CaO promoters produce the basic property of the Ni catalyst, whereas La_2O_3 enhances the acidity of the catalyst. The difference in the surface acid−base characteristics of promoted catalysts can be explained by the distribution of metal oxide promoters in carbon pores. It has been shown that most of the basic CaO are deposited at the outer surface layer and MgO is more distributed in the inner pores. This resulted in the basicity order of the catalysts as Ni/CaO−AC > Ni/MgO−AC > Ni/AC. For the Ni/La_2O_3−AC catalyst, it showed an acidic property because the acidic La_2O_3 was also deposited on the carbon surface.

A conventional X-ray diffraction line broadening (XRDLB) method was used to calculate the metallic crystallite diameter. These results are listed in Table 4. It is seen that the metal diameter of promoted

Table 3. Mass Ratios of Ni or Promoter (MO, M = Mg, Ca, La) to Carbon on the Surface and in Bulk

catalyst	$(Ni/C)_{xps}$ (wt %)	$(MO/C)_{xps}$ (wt %)	$(Ni/C)_b$ (wt %)	$(MO/C)_b$ (wt %)	$(Ni/C)_{xps}/(Ni/C)_b$	$(MO/C)_{xps}/(MO/C)_b$
Ni/AC	5.0		5.9	0	0.85	
Ni/MgO−AC	4.4	0.3	5.9	2.8	0.74	0.11
Ni/CaO−AC	5.8	2.9	7.1	2.4	0.82	1.21
Ni/La_2O_3−AC	1.5	8.4	6.1	2.4	0.24	3.50

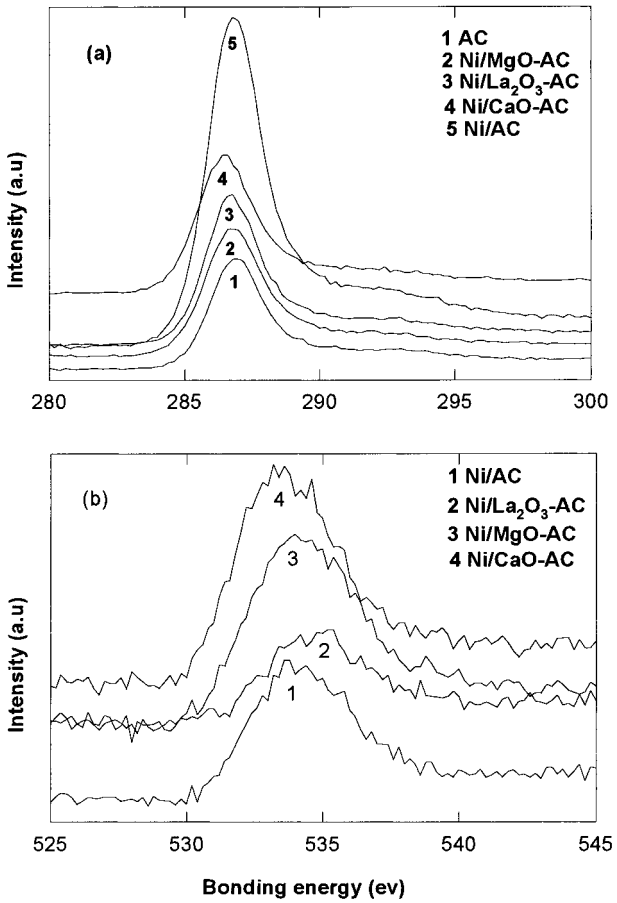

Figure 4. XPS spectra of C 1s and O 1s of various nickel−carbon catalysts. (a) C 1s; (b) O 1s.

Table 4. Average Mean Crystallite Diameter (D_{XRD}) of the Active Component in Various Catalysts

catalyst	D_{XRD} (nm)	catalyst	D_{XRD} (nm)
Ni/AC	22.8	Ni/CaO−AC	10.3
Ni/MgO−AC	10.9	Ni/La_2O_3−AC	21.8

catalysts is lower than that of the unpromoted catalyst, demonstrating that the addition of promoters generally increases the metal dispersion. The degree of dispersion of Ni is in the order of Ni/CaO−AC > Ni/MgO−AC > Ni/La_2O_3−AC > Ni/AC.

Metal dispersion in the support is strongly dependent on the distribution of the active phase within the support and on the type and degree of interaction reached. From the XPS results it is seen that Ni can be more uniformly distributed in the pores of promoted catalysts. Ni/La_2O_3−AC has a lower $(Ni/C)_{xps}/(Ni/C)_b$ ratio. However, its dispersion is enhanced a little. This may be due to the different degrees of interaction of Ni and carbon by addition of promoter oxide. During the reduction stage, heat treatment resulted in the decomposition of the less stable oxygen complexes (acidic groups). Thus, the mobility of nickel on the support surface may be favored and as a consequence the agglomeration of nickel particles enhanced. This effect has also been observed in Pt/AC (Suh et al., 1993) and Mo/AC systems (Solar et al., 1992).

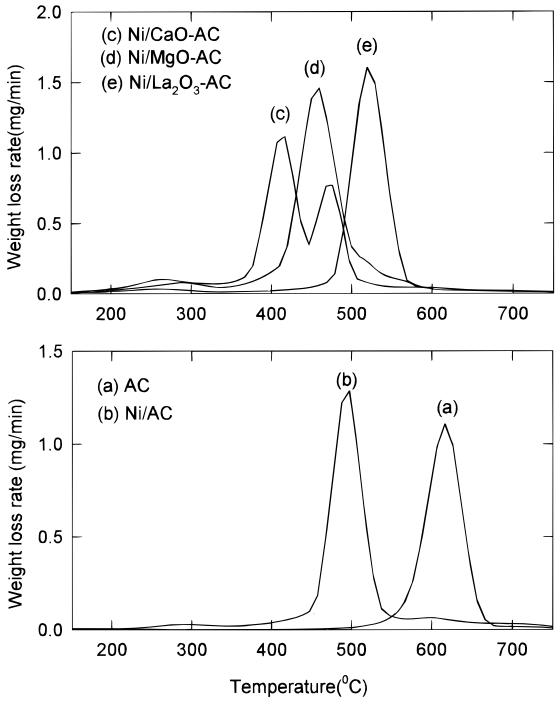

Figure 5. Temperature-programmed oxidation (TPO) profiles of the support and catalysts in a TGA.

3.3. Thermogravimetric Analysis (TGA). Figure 5 shows the oxidation rates of the carbon support, unpromoted and promoted Ni catalysts in air. It is seen that there are two peaks in Ni catalysts, which is different from that of the carbon support. The first peak occurring at 200−350 °C is indicative of nickel nitrate decomposition to nickel oxide (Wang and Lu, 1997). The second peak corresponds to carbon oxidation. It is noted that oxidation reactivities of Ni catalysts are higher than that of the carbon support, which is attributed to the catalytic property of Ni on gasification of carbon. Promoters have some different influences on the gasification activity. MgO and CaO increase the carbon gasification reactivity. However, CaO-promoted catalyst shows a two-tier type of activity. The third peak of oxidation profile for the Ni/CaO−AC catalyst may be due to the reaction between Ca salt and carbon forming $CaCO_3$ and then decomposing to the oxide (CaO) (Haga et al., 1992). La_2O_3 promoter results in a higher ignition temperature than that of unpromoted Ni catalyst, which represents a lower oxidation reactivity for Ni/La_2O_3−AC.

Parker et al. (Rakszawski and Parker, 1964; Heintz and Parker, 1966) have studied the effect of elements and oxides on graphite oxidation in air and found that most additives behaved as catalysts. However, some showed inhibiting properties. In Table 5 are shown the activation energies of oxidation for metal−carbon systems. It is seen that Mg, Ca, and Ni have catalytic properties for the carbon−air oxidation, whereas La shows an inhibition effect on this reaction.

Table 5. Activation Energy for the Oxidation of Graphite in the Presence of Metal in Air (Heintz and Parker, 1966)

system	E_a (kcal/mol)	system	E_a (kcal/mol)
C	48.8	Ba-C	<10
Mg−C		Ni−C	46.2
Ca−C	25.0	La−C	57.3
Sr-C	<20		

Table 6. Temperature and Activated Energies for Oxidation of Carbon-Supported Catalysts

	temperature (°C)	E_a (kcal/mol)
AC	585−645	63.7
Ni/AC	465−505	61.9
Ni/MgO−AC	375−425	36.7
Ni/CaO−AC	430−480	30.2
Ni/La_2O_3−AC	490−550	59.5

Activated energies for these reactions were calculated based on the carbon conversion between 0.2 and 0.8 using equation

$$dX/dT = Ae^{-E_a/RT}(1 - X) \quad (1)$$

where $X = (W_0 - W)/(W_0 - W_f)$, W_0 is the initial weight, W is the weight of unreacted carbon, and W_f is the ash weight at the end of the reaction. It is found that the oxidation reaction is of first order. Activation energies for carbon support or Ni−C catalysts are of the same order of magnitude. The activated energies for promoted Ni/C catalysts are much lower, particularly for Ni/MgO−AC and Ni/CaO−AC catalysts (Table 6). The activation energies are larger than those reported by Parker et al. (Table 5) for graphites.

The gasification of carbon is normally dependent on (1) the acid−base property of carbon, (2) the interaction between the metal and carbonaceous materials, and (3) the gaseous atmosphere. It has been reported that the more acidic the carbon, the higher the ignition temperature of carbon. Nickel species are more strongly bound to basic sites than to acidic sites, resulting in stronger metal−support interaction. Such a bonding inhibits the role of nickel species as a catalyst (Noh and Schwarz, 1991). From the XPS results it has been demonstrated that the order of basicity of Ni catalysts is as follows: Ni/CaO−AC > Ni/MgO−AC > Ni/AC > Ni/La_2O_3−AC. Therefore, the variation in the trend of ignition temperature is closely related to the basicity order. This confirms the conclusion deduced by Noh and Schwarz (1991).

Some researchers recently reported that there were two kinds of nickel−carbon interactions. One is a Ni−(O)−C type of interaction which is responsible for the lower temperature catalysis of nickel at 400−700 °C. This is accompanied by the thermal desorption of CO from the oxygen groups remaining on the carbon at 650 °C. The other is the dissolution of carbon into nickel followed by internal diffusion and is likely to become evident at 600 °C (Baker and Sherwood, 1981; Yang et al., 1990). From Figure 5 we can find that all nickel catalysts react with air in the temperature of 350−600 °C, which seems to indicate that the first metal−support interaction prevails in the oxidation process. The oxygen in air is adsorbed on the porous solid. The metal ion serves as an initial oxygen acceptor and then transfers the oxygen directly to a carbon, leading to carbon oxidation. Alkaline-earth metal oxides (MgO and CaO) have stronger electropositive properties, which makes them act as electron acceptors in carbon oxidation. Hence, MgO- and CaO-promoted catalysts showed higher oxidation reactivity. The inhibition of carbon oxidation may have two possible reasons. The inhibitors can remove free electrons from the active sites with the result that the active sites are no longer capable of reacting. In addition, the inhibiting molecules may cover the active sites so that the reactant is not able to attack the surface. Therefore, the inhibiting effect of La_2O_3 is possibly due to the coverage of the active sites because most of La_2O_3 deposited at the outer layer of carbon and thus prevented the contact between carbon and oxygen.

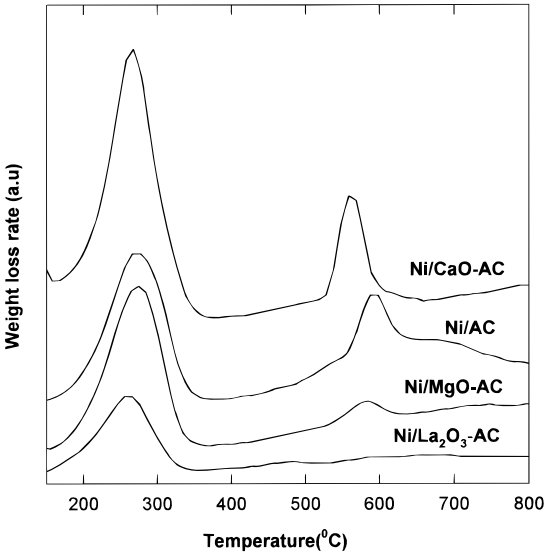

Figure 6. Rates of thermal decomposition of various nickel catalysts at N_2 in a TGA.

In order to study the behavior of the precursor and support as well as their interaction during calcination, thermal decomposition experiments were conducted in a TGA under a N_2 atmosphere. In Figure 6 is illustrated the thermal decomposition of catalysts in nitrogen. There are two peaks occurring in the temperature ranges of 150−350 and 500−650 °C for Ni/AC, Ni/MgO−AC, and Ni/CaO−AC catalysts. However, for Ni/La_2O_3−AC there is only one peak appearing in the range of 150−350 °C. The lower temperature peak corresponds to nickel nitrate decomposition to nickel oxide on the carbon support whose decomposition temperature is lower than that of nickel salt (280−400 °C) (Haga et al., 1992; Wang and Lu, 1997). It has been reported that nickel oxide may interact with carbon to produce metallic nickel around 500−600 °C (Gandia and Montes, 1994; Wang and Lu, 1997). Therefore, the second peak is possibly attributed to the redox reaction between metal salt and the carbon.

In order to prove that there is a redox reaction occurring at 500 °C, XRD measurements were conducted. In Figure 7 are shown the XRD patterns of the support and Ni/C catalysts heat-treated at 300 and 500 °C. It is seen that the XRD pattern of the support is indicative of a typical amorphous carbon. The Ni/C catalyst XRD patterns are much similar to that of the support. However, peaks corresponding to nickel oxide and nickel appear when heat-treated in N_2 at different temperatures. At 500 °C nickel was detected on the catalyst surface, which indicates that a redox reaction occurred between nickel oxide and carbon. Due to the possible contamination and some oxidation on the catalyst surface when samples were prepared for XRD measurements, the nickel oxide peak still existed.

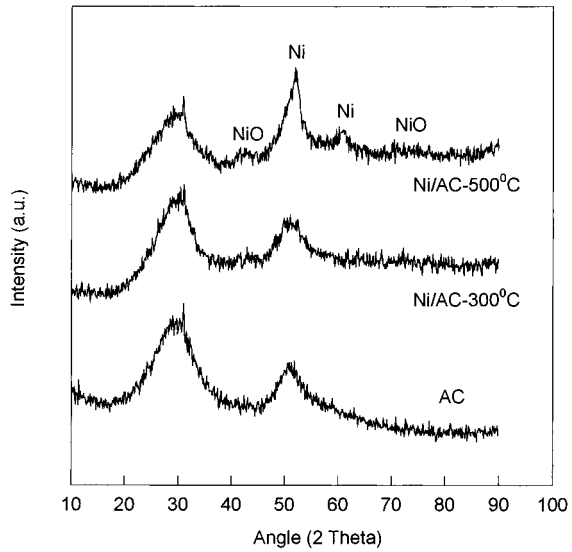

Figure 7. XRD patterns of the support and catalysts heat-treated at different temperatures.

Table 7. Weight Loss in the Redox Reaction for Various Nickel Catalysts

catalyst	weight loss (%)	catalyst	weight loss (%)
Ni/AC	3.38	Ni/CaO−AC	2.88
Ni/MgO−AC	3.28	Ni/La_2O_3−AC	1.25

Hence, it is difficult to compare the reduction extent quantitatively from XRD measurements.

It is seen that promoters have some influence on nickel salt decomposition on carbon. The temperature for nickel salt decomposition on promoted catalysts is lower than that for the unpromoted catalyst. This means that addition of promoters makes the decomposition much easier. In addition, they can also affect the reactivity between nickel oxide and carbon. It is seen in Figure 6 that CaO and MgO lower the peak temperature (T_{peak}) of the redox reaction in promoted catalysts to below that of the unpromoted catalyst. This means that promoters MgO and CaO decrease the temperature of the redox reaction; in other words, the redox activities of MgO- and CaO-promoted catalysts are higher.

As discussed in the previous section, the interaction of the metal and support may be responsible for the redox reaction. However, it is unlikely that the oxygen is transferred from the gaseous atmosphere to the support as in the oxidation process. It is possible that the oxides resulting from the nitrate decomposition transfer their oxygen atoms to the support.

In order to evaluate the weight loss due to the redox process, the decomposition curve for the carbon support has been subtracted from that of the Ni/AC catalyst and the corresponding weight changes between 500 and 650 °C have been calculated (Table 7). It is seen that promoted catalysts show less weight losses than that of the unpromoted catalyst. Among the three promoters, La_2O_3 resulted in the lowest weight change during the redox reaction, indicating that Ni/La_2O_3−AC has the lowest redox activity. During the impregnation process, promoters partly cover the surface of carbon, thus preventing the direct contact between nickel and carbon and leading to weaker interaction between nickel salt and carbon. From the XPS results, it is known that most of the La_2O_3 promoter is deposited on the outer surface of carbon. This may prevent the interaction between carbon and nickel oxide to the greatest extent.

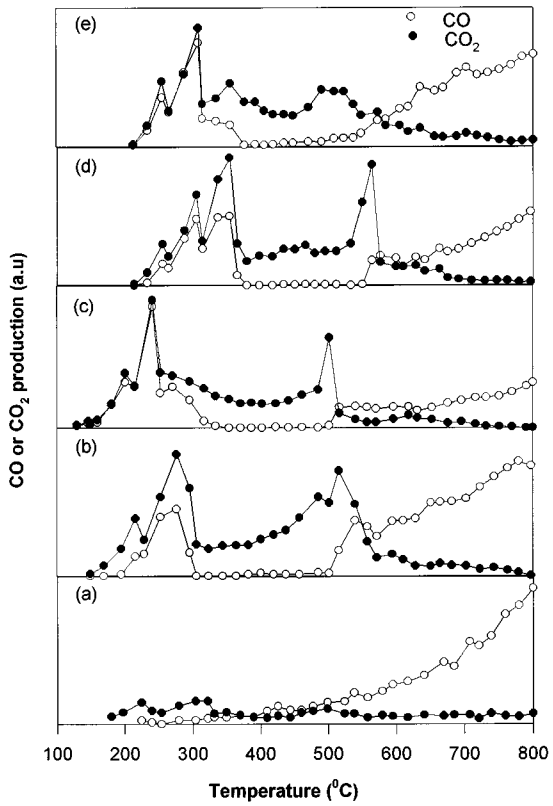

Figure 8. CO and CO_2 evolution profiles for the support and various Ni/AC catalysts: (a) AC; (b) Ni/AC; (c) Ni/CaO−AC; (d) Ni/MgO−AC; (e) Ni/La_2O_3−AC.

Therefore, it will be difficult for nickel oxide to be reduced in the Ni/La_2O_3−AC catalyst.

3.4. Temperature-Programmed Desorption (TPD). TPD profiles of the support and Ni-based catalysts are shown in Figure 8. The carbon support exhibits three CO_2 peaks in the ranges of 200−250, 250−350, and 400−550 °C, respectively. No CO peak was detected for the carbon support. This means that acidic groups on the support could be easily decomposed, but the basic groups are very stable. The profiles for the impregnated carbons show quite different CO and CO_2 evolution behaviors. The amounts of oxygen groups evolved increased when impregnated with nickel nitrate and other salts. The unpromoted and MgO- and CaO-promoted carbons show two more peaks in CO profiles in the temperature ranges of 100−300 and 500−600 °C, while the La_2O_3-promoted catalyst has only one peak in its CO profile occurring at 100−300 °C. Similarly, in CO_2 profiles, unpromoted and MgO- and CaO-promoted carbons show more intense peaks especially at 480−550 °C. However, the La_2O_3-promoted catalyst shows a small peak at 400−500 °C.

Comparing the TPD profiles and weight loss rate profiles in N_2 (Figure 6), it is seen that they show much similar patterns. Lower temperature peaks in the TPD profiles demonstrate nitrate decomposition ($Ni(NO_3)_2 \rightarrow$ NiO) and higher temperature peaks are indicative of the redox reaction (NiO → Ni). It is noted that the intensities of peaks in CO and CO_2 profiles show that the redox reaction occurring on Ni/AC, Ni/MgO−AC, and Ni/CaO−AC catalysts was strong while the extent of reaction was lower for Ni/La_2O_3−AC. The peaks occurring around 500 °C in the TPD profiles also show that both CO and CO_2 were produced by the redox reaction. Hence, it is proposed that the redox process happened simultaneously as follows:

$$NiO + C \rightarrow Ni + CO \quad (2)$$

$$2NiO + C \rightarrow 2Ni + CO_2 \quad (3)$$

4. Conclusions

(1) Impregnation produces a partial blocking of the porosity of the carbon support. Ni salt is generally deposited in micropores. Alkaline-earth metal oxides (MgO, CaO) and a rare-earth oxide (La_2O_3) block more mesopores. Addition of promoted oxide enhances Ni diffusion into the micropores. XPS measurements show that, in the impregnation process, nickel salt can be dispersed homogeneously in the carbon pores. For promoters, their distributions in activated carbon vary, resulting in different surface acid−basicity properties of the catalyst. Magnesium salt may be homogeneously distributed in the carbon pores, whereas calcium and lanthanum salts are concentrated on the outer surface.

(2) Unpromoted nickel catalyst may react with carbon in an inert atmosphere at higher temperatures as a redox reaction. Promoters decrease the redox extent of Ni catalysts and increase the reaction reactivity by lowering the reaction temperature.

(3) Promoters have some different influences on the gasification activity of carbon. MgO and CaO increase the carbon oxidation reactivity, whereas La_2O_3 decreases the oxidation reactivity.

(4) Addition of MgO and CaO promoters increases not only the dispersion of nickel crystallites but also the surface basicity. Although addition of the La_2O_3 promoter increases the dispersion of nickel crystallite, it increases the surface acidity.

Acknowledgment

We thank Dr. B. J. Wood of Department of Chemistry at University of Queensland for his assistance with XPS measurements. We also thank Dr. H. Y. Zhu for his valuable discussions on pore structure. Partial support from the Australian Research Council (ARC) is gratefully acknowledged as well.

Literature Cited

Baker, R. T. K.; Sherwood, R. D. Catalytic gasification of graphite by nickel in various gaseous environments. *J. Catal.* **1981**, *70*, 198−214.

Bekyarova, E.; Mehandjiev, D. Studies of Ni-impregnated active carbon. Part I. Effect of thermal treatment on the texture of active carbon and the state of the active phase. *J. Colloid Interface Sci.* **1996**, *179*, 509−516.

Domingo-Garcia, M.; Fernandez-Morales, I.; Lopez-Garzon, F. J. Activated carbons as supports for nickel catalysts. *Appl. Catal.* **1994**, *112*, 75−85.

Gandia, L. M.; Montes, M. Effect of thermal treatment on the properties of nickel and cobalt activated-charcoal-supported catalysts. *J. Catal.* **1994**, *145*, 276−288.

Haga, T.; Ozaki, J. I.; Suzuki, K.; Nishiyama, Y. Role of MgO and CaO promoters in Ni-catalysed hydrogenation reaction of CO and carbon. *J. Catal.* **1992**, *114*, 107−117.

Heintz, E. A.; Parker, W. E. Catalytic effect of major impurities on graphite oxidation. *Carbon* **1966**, *4*, 473−482.

Kaneko, K.; Ishii, C. ; Ruike, M.; Kuwabara, H. Origin of superhigh surface area and microcrystalline graphitic structures of activated carbons. *Carbon* **1992**, *30*, 1075−1088.

Lemaitre, J. L.; Menon, P. G.; Delanny, F. The Measurement of Catalyst Dispersion. In *Characterization of Heterogeneous Catalysts*; Delanny, F., Ed.; Marcel Dekker: New York, 1985.

Molina-Sabio, M.; Perez, V.; Rodriguez-Reinoso, F. Impregnation of activated carbon with chromiun and copper salts: effect of porosity and metal content. *Carbon* **1994**, *32*, 1259−1265.

Noh, J. S.; Schwarz, J. A. Relationship between metal ion adsorption and catalytic properties of carbon-supported nickel catalysts. *J. Catal.* **1991**, *127*, 22−33.

Rakszawski, J. F.; Parker, W. E. The effect of group IIIA−VIIA elements and their oxides on graphite oxidation. *Carbon* **1964**, *2*, 53−64.

Rodriguez-Ramos, I.; Guerrero-Ruiz, A.; Fierro, J. L. G. Effect of oxide promoters on the surface characteristics of carbon-supported Co and Ru catalysts. *Appl. Surf. Sci.* **1989**, *40*, 239−247.

Solar, J. M.; Derbyshire, F. J.; de Beer, V. H. J.; Radovic, L. R. Effect of surface and structural properties of carbons on the behavior of carbon-supported molybdenum catalysts. *J. Catal.* **1991**, *129*, 330−342.

Suh, D. J.; Park, T. J.; Ihm, S. K. Effect of surface oxygen groups of carbon supports on the characteristics of Pd/C catalysts. *Carbon* **1993**, *31*, 427−435.

Tripathi, V. S.; Ramachandran, P. K. Studies on metal impregnated activated carbon: complete pore structure analysis. *Carbon* **1982**, *20*, 25−27.

Wang, S.; Lu, G. Q. Effects of acidic treatments on the pore and surface properties of Ni catalysts and the activated carbon support. *Carbon*, submitted for publication.

Yang, R. T.; Goethel, P. J.; Schwarz, J. M.; Lung, C. R. F. Solubility and diffusivity of carbon in metals. *J. Catal.* **1990**, *122*, 206−210.

Zhu, H. Y.; Lu, G. Q.; Maes, N.; Vansant, E. F. An improved MP-method for the determination of pore size distribution of porous materials. *J. Chem. Soc., Faraday Trans.* **1997**, *93*, 1417−1424.

Received for review May 21, 1997
Revised manuscript received August 26, 1997
Accepted August 29, 1997[⊗]

IE9703604

[⊗] Abstract published in *Advance ACS Abstracts*, November 1, 1997.